Breast Density Assessment in Adolescent Girls Using Dual-Energy X-ray Absorptiometry: A Feasibility Study

John A. Shepherd,[1] Serghei Malkov,[1] Bo Fan,[1] Aurelie Laidevant,[1] Rachel Novotny,[2,3] and Gertraud Maskarinec[4]

[1]Musuloskeletal and Quantitative Imaging Research Group, Department of Radiology, University of California at San Francisco, San Francisco, California; [2]Kaiser Permanente, Center for Health Research Hawaii; [3]Department of Human Nutrition, Food and Animal Sciences, College of Tropical Agriculture and Human Resources; and [4]Cancer Research Center, University of Hawaii, Honolulu, Hawaii

Abstract

Breast density, the radiographically opaque fraction of the breast in a mammogram, is one of the strongest biomarkers of breast cancer risk. However, younger populations do not typically have mammograms due to radiation concerns. This study explored a commercially available dual-energy X-ray absorptiometer (DXA) system as a low-dose method to measure breast fibroglandular density in adolescent girls. Eighteen girls (13-14 years old) indicated their breast development according to Tanner and underwent three dedicated DXA scans, two of their left and one of their right breasts. Total projected breast area was manually delineated on each image and percent fibroglandular volume density (%FGV), absolute fibroglandular volume (FGV), total breast area, and volume were computed. It was possible to image breasts representing all five Tanner stages; %FGV ranged from 31.9% to 92.2% with a mean of 71.1 ± 14.8%, whereas FGV ranged from 80 to 270 cm^3 with a mean of 168 ± 54 cm^3. Left and right breast %FGV were highly correlated (r_p = 0.97, P < 0.0001) and of the same magnitude (P = 0.18). However, left total volume and FGV were larger than the right by 38 cm^3 (P = 0.04) and 19 cm^3 (P = 0.02), respectively. Total volume and FGV increased by Tanner stage, whereas %FGV did not. Our method had excellent precision for %FGV and moderate precision for FGV (root mean square SDs of 2.4% and 16.6 cm^3). These pilot data indicate that dedicated DXA breast scans may be useful in studies exploring breast density in girls. (Cancer Epidemiol Biomarkers Prev 2008;17(7):1709–13)

Introduction

Breast density, measured as the ratio of radiographically dense tissue area to the total breast area in a mammogram, has been shown in numerous studies to be one of the strongest biomarkers of breast cancer risk (1). Breast density is also correlated with other histologic features related to increased breast cancer risk (2). Women in mammography screening populations with high breast density (the top 25% of the density distribution) are at three to four times higher risk of developing breast cancer compared with women with low breast density (the lower 25% of the density distribution; ref. 3). Given that there is a great need for surrogate markers to predict breast cancer risk to test promising preventive treatments, measures of breast density have the potential to be powerful predictors of cancer risk. To date, breast density has not been used for individual risk prediction but can be measured with mammograms, using either a semiquantitative classification system [Wolfe criteria (4) or BIRADS scores (5)], or as percent density, which is the ratio of the area of mammographically dense breast relative to the total projected breast area in a mammogram (6, 7). However, these methods quantify density as a projected area and only use two-dimensional image information. Kopans (8) pointed out that there can be substantial error when measuring a three-dimensional property, like breast density, with a two-dimensional method. Thus, we approached the measure of breast density using the technique dual-energy X-ray absorptiometry (DXA), which has the capability to measure the volume and mass of dense tissue. DXA is a low-dose quantitative method first developed for measuring bone density and mass to diagnose osteoporosis. However, the technique is also widely used to assess whole body soft tissue composition as percent fat mass. DXA systems operate at much higher X-ray tube voltage settings than standard mammography (70-140 versus <40 kVp, respectively), yet lower in patient dose because it is used to quantify mass over large areas. DXA is commonly used to measure whole body percent fat and bone mass in pediatric studies (9). We developed a dedicated breast DXA scan protocol that exposes subjects to an ~10 times lower dose than a single mammogram (15 μSv for a breast DXA versus 150 μSv for a screening mammogram; ref. 10).

We have previously reported on recalibration of a DXA system to measure percent breast fibroglandular density and quantified the precision of accuracy in excised cadaver breasts (11) and in a small population of women (12). Our earlier findings showed that the DXA measures are very precise with repeatability of the percent fibroglandular volume (%FGV) to 2%. However,

Received 1/3/08; revised 4/30/08; accepted 5/4/08.

Grant support: The University of Hawaii Clinical Research Center, supported by grant P20 RR11091 from the National Center for Research Resources, NIH.

Requests for reprints: John A. Shepherd, Department of Radiology, Box 0946, University of California at San Francisco, San Francisco, CA 94143-0946. Phone: 415-502-6732; Fax: 415-502-7671. E-mail: john.shepherd@radiology.ucsf.edu

Copyright © 2008 American Association for Cancer Research.

doi:10.1158/1055-9965.EPI-08-0006

Downloaded from cebp.aacrjournals.org on January 16, 2021. © 2008 American Association for Cancer Research.

there is great interest in studying cancer biomarkers in early life, such as breast density in girls. Little is known about when a girl reaches her peak breast density and how density relates to genetics and early life habits such as diet. In this article, we report on the characteristics of our DXA method to measure breast fibroglandular density in adolescent girls at different pubertal stages of breast development.

Materials and Methods

Subjects. Eighteen girls (13-14 years old) were recruited as a convenience sample from the Adequate Calcium Today study (13), a multisite trial that examined the influence of a multimedia intervention on calcium intake and bone health of sixth grade girls (principal investigator: D. Savaiano). These subjects underwent a full-body DXA scan and consented to be recontacted. Therefore, the girls and their families were familiar with DXA scans and understood the very low level of exposure to radiation. The project was approved by the Committee on Human Studies at the University of Hawaii and by the Institutional Review Board of Hawaii Pacific Health, where the DXA machine is located. All girls signed an assent form and their parents signed an informed consent form. After weight and height measurements and confirming the absence of pregnancy by a urine test, participants underwent two dedicated DXA scans of their left breast and one of their right breast.

DXA Data Acquisition. All scans were acquired using the research scan protocol and software version 9.3 on a GE Lunar Prodigy Bone Densitometer (GE Healthcare). The scan options were set to research mode, standard X-ray technique, and scan width equal to 20 cm and length of 30 cm. The pixel dimensions were 1.0×1.5 mm^2. After removing all clothing, and wearing cotton hospital gowns, the participants were positioned for dedicated decubitus mediolateral scanning of each breast. For imaging the left breast, the girls lay on their left side with their left arm resting below their head. Their left breast rested on the DXA surface and their right hand was used to hold their right breast out of the DXA scanning path. Standard radiolucent positioning wedges were used to support their back as well as the left breast to put the nipple in profile. The gown was pulled to lay smoothly over the image area with few folds. No breast compression was used. Each scan was manually stopped after scanning the entire breast length to minimize dose. After scanning the left breast, the girls were asked to roll over and were repositioned to scan the right breast. Lastly, the subjects were asked to get up and off the DXA machine, and then to remount the DXA, when they were repositioned for a second DXA scan of the left breast. The repositioning was to simulate the differences that would occur between repeated examinations. The X-ray dose per breast scan was estimated to be 15 μSv. A single DXA technologist performed the DXA scans for all participants.

Low-energy and high-energy attenuation images were saved for each scan using the options available from GE Lunar for the research scan mode. Data analysis was done on the University of California at San Francisco Breast Density Workstation (14). The scans were calibrated to a two-compartment model of fat (steric acid) and fibroglandular tissue density using a variety of custom phantoms as described previously (11). Briefly, calibration phantoms of a known range of breast composition and thickness are scanned. A ''ratio value'' (R value) is defined as the ratio of the low-energy to high-energy attenuation for density and thickness. The paired R value and high-energy attenuation value are unique for each density and thickness. We define two polynomial functions to convert the R values and high-energy attenuations to either %FGV or breast thickness for each pixel. The dense breast volume in pixels is the product of the %FGV and the calculated volume of tissue in the pixel (thickness $\times$ pixel area). Total projected breast area was manually delineated on each image in a workstation with the use of a mouse as previously described (11). The whole breast density (%FGV) was computed as the sum of dense fibroglandular volume (FGV) in cubic centimeters divided by the total breast volume (sum of all pixel volumes) times 100.

For quality assurance purposes and to assess the intrinsic repeatability of the density measurements using the GE Lunar Prodigy DXA machine, we performed three scans of the density step phantom everyday for 2 wk. The phantom varied in thickness (2, 10, and 20 cm) and contained three %FGV values of 28%, 65%, and 100%.

Tanner Staging. All girls in the study were shown a diagram of breast development depicting the five Tanner stages (15) of breast development (Fig. 1) and were asked to select their current appearance. This method has been shown to be valid when compared with clinical staging done by health professionals (16).

The five stages describing the development of the breast by Tanner are as follows:

1. Same as in childhood; small elevated nipple with no significant underlying breast tissue.
2. Breast buds become visible. There is elevation of the breast and nipple as a small mound; the areola begins to enlarge. Milk ducts inside the breast begin to grow.
3. Further enlargement and elevation of the breast and areola occurs. The areola begins to darken in color. The milk ducts give rise to milk glands that begin to grow.
4. The areola rises above the rest of the breast and forms a secondary mound.
5. Only the nipple projects although in some woman the areola continues to form a secondary mound.

Statistical Analysis. All data management and analyses were done using the SAS statistical software package, version 9 (SAS Institute, Inc., 2001). *In vivo* repeatability was assessed using the repeat DXA scans of the left breast. The repeatability (precision) of the measures was calculated as SD and percent coefficient of variation (%CV) for each subject. For a representative precision value of the population, we define precision as the root mean square SD (RMS SD) and root mean square percent coefficient of variation (RMS %CV) as done commonly elsewhere (17).

Downloaded from cebp.aacrjournals.org on January 16, 2021. © 2008 American Association for Cancer Research.

$$\text{RMS SD} = \sqrt{\sum_{j-1}^{m} \frac{\text{SD}_j^2}{m}} \qquad (A)$$

and

$$\text{RMS \%CV} = \sqrt{\sum_{j=1}^{m} \frac{\%\text{CV}_j^2}{m}} \qquad (B)$$

where SD_j and CV_j represent the values for the jth participant, and m is the total number of participants in the precision study. Comparisons between left and right breast measures were done by calculating the Pearson's Correlation coefficient (r_p). Mean levels of breast total volume, projected area, %FGV, and FGV tissue were computed as a function of Tanner pubertal breast stage, and the associations to Tanner stage described by the Spearman's rank correlation coefficient (r_s). The density step phantom was analyzed using a template of seven regions of interest. The stability of the DXA system was determined by plotting the phantom results over time and checking for breaks in the calibration using standard process control methods and Shewhart rules (18).

Results

This study included 18 girls of ages 13 to 14 years. Of these, 11 reported Japanese ancestry, 3 were mixed Japanese/Chinese, 2 were Chinese, and 1 each reported Filipina and Korean ethnicity. All girls, except one, had reached menarche. The mean body weight was 47.4 $\pm$ 7.1 kg. The breast development in the girls was classified into the following Tanner stages: one as stage 1, three as stage 2, eight as stage 3, five as stage 4, and one as stage 5.

The DXA images showed the breast tissue separate from the pectoral muscle and rib cage. However, there was not much detail in the fibroglandular tissue. Figure 1 shows typical scans as a function of Tanner pubertal stage. Left and right measures for %FGV, FGV, total area, and total volume were all highly correlated (Table 1). Total breast volume and FGV are larger, on average, for left than for right breasts (P = 0.04 and P = 0.02, respectively). Breast volumes (mean of right and left) ranged from 113 to 670 cm^3 with a mean of 254 cm^3. FGV ranged from 80 to 270 cm^3 with a mean of 168 $\pm$ 54 cm^3. Percent FGV ranged from 32% to 92% with a mean of 71 $\pm$ 14.8%. Body mass index (BMI) showed a significant relation with %FGV (r_p = -0.68, P = 0.003) and total volume (r_p = 0.56, P = 0.02) but not with FGV (P = 0.95).

As shown in Fig. 2, the total breast volume and FGV increased significantly by Tanner stage (P = 0.003) whereas %FGV showed an inverse trend but was not statistically significant (P = 0.90). The respective FGV means by Tanner stage were 104, 124, 161, 210, and 214 cm^3.

The precision is shown both as RMS CV and RMS SD for %FGV and FGV in Table 1. The RMS SD was 2.4% for %FGV and 16.6 cm^3 for FGV. These values are comparable to the phantom precision values that ranged from 1.5% (10 cm in thickness and 100% composition) to 2.4% (2 cm in thickness and 28% composition). There were no observed changes in the systems calibration over time observed from the density step quality control phantom.

Discussion

Our pilot study to test the feasibility of using a standard bone densitometer to capture images of adolescent girls (Fig. 1) found that it was possible to image all Tanner stages and that breast volume and FGV density were related to Tanner stages. The total and dense volumes of the breast increased by Tanner stage, whereas we found no relation between %FGV and Tanner stage. However, we only had one girl with Tanner 1 and Tanner 5. Thus, our ability to make definitive statements about density and pubertal development was limited.

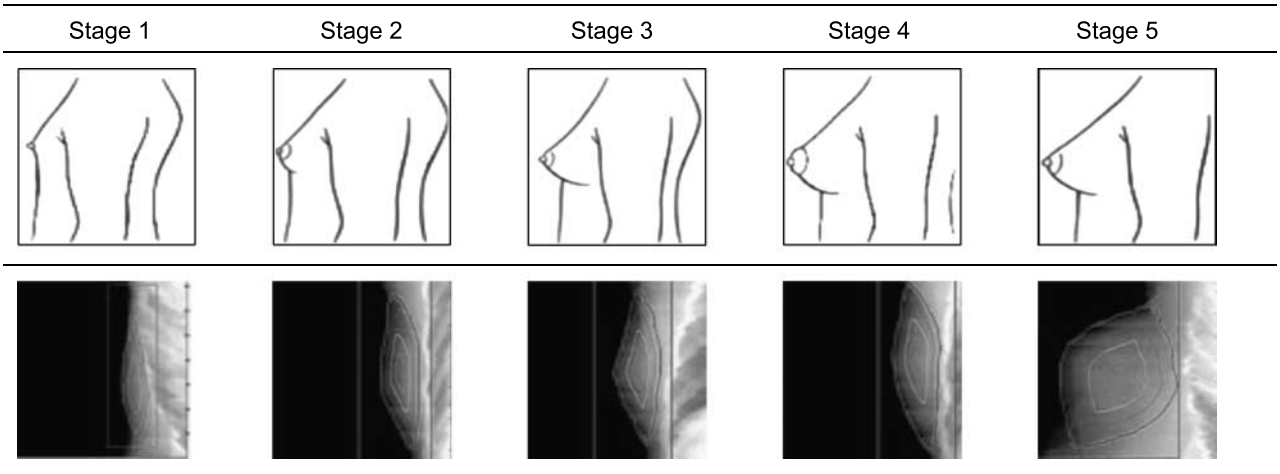

Figure 1. Breast pubertal stages according to Tanner with the corresponding DXA image. The total breast area is shown as the largest region of interest around the breast (*blue*).

Downloaded from cebp.aacrjournals.org on January 16, 2021. © 2008 American Association for Cancer Research.

Table 1. Summary of DXA measures for left and right breasts

Breast measure	Mean (min, max)	Difference	r_p*	RMS %CV (RMS SD)
Total volume, left (cm^3)	272.3 (121.0, 817.9)	38 †	0.91 †	12.2 (30.7)
Total volume, right (cm^3)	234.0 (104.2, 522.3)			
Total area, left (cm^2)	34.8 (16.5, 83.4)	4.2 †	0.86 †	8 (3.7)
Total area, right (cm^2)	30.6 (13.8, 54.7)			
FGV, left (cm^3)	177.8 (85.7, 287.1)	19 †	0.85 †	12.2 (15.8)
FGV, right (cm^3)	158.8 (75.1, 292.9)			
%FGV, left	70.5 (32.5, 91.4)	−1.3	0.97	N/A ‡ (2.4)
%FGV, right	71.7 (31.2, 92.2)			

*Pearson's correlation coefficient.
† $P < 0.05$.
‡ Note that taking the percent of a percent value is not standard practice.

The repeatability was high for %FGV (2.5%) but only moderate for FGV (12%). In our previous work with women, we found the repeatability of %FGV from similar DXA scans to be 1.2% (14). We believe that some of this difference in precision between girls and women to be breast size, but we plan to further develop and standardize subject positioning and automated outlining of the breast area to improve the precision on girls. A sign of overall accuracy was that the percentage of fat using the GE Lunar DXA analysis was highly correlated with the breast phantom percentage fibroglandular density reported by the phantom's manufacturer (r >0.998).

BMI was inversely correlated to %FGV. Other studies have also found breast density measured from mammograms inversely corrected to BMI for postmenopausal women (19). However, the correlation of BMI and breast density has not precluded breast density as an independent risk factor. Barlow showed in a multivariate model that BMI and breast density were both strongly associated with breast cancer in postmenopausal women (20). After controlling for breast density, breast cancer risk was 47% higher for women with a BMI of ≥35 when compared with women with a BMI of <25. At the same time, the risk association to breast density was 3-fold higher for women in the highest breast density category compared with the lowest.

These results are comparable to the DXA study among 17 women (14) that also reported a high correlation for left and right measures. We found the left breasts to be, on average, higher in total volume and FGV than the right breasts. This is consistent with the findings in women that left breasts are larger in general (21). Hussain et al. (22) found that the average difference was 39.7 cm^3 in 22 women using a magnetic resonance imaging technique. Interestingly, we observed a difference of 38 cm^3 although our sample was very small. A lower percentage density with larger breasts is consistent with the findings in women; on average, larger breasts have more fatty tissue and lower percent density (23). The increase in FGV with Tanner stage is also consistent with developing breasts, although our study was limited by few girls in the Tanner 1 and Tanner 5 categories.

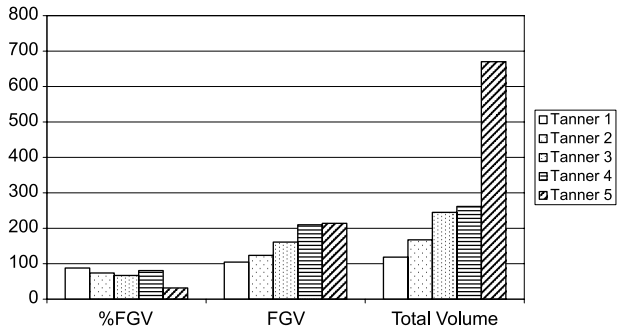

Figure 2. Mean breast density measures by Tanner stage.

We also showed in this study that our DXA breast scanning technique is generalizable across DXA hardware. This study was done on a GE Prodigy whereas our previous work was on a Hologic Delphi/A. However, the analysis algorithms and calibration standards were the same. Thus, we would expect indistinguishable results if the present study were to be reproduced on a Hologic system.

Although these preliminary findings look promising, data on a larger sample of girls and a more thorough understanding of breast density are necessary before DXA scanning can be applied in longitudinal or intervention studies. A method to monitor breast composition in young women and girls is currently not available because the risk of X-ray based mammograms outweighs potential benefits in that age group (24). Novel techniques to obtain images of the developing breast are also of interest because there is an interest to develop low-radiation methods for adult women to monitor breast density for individualized risk prediction (25). Magnetic resonance imaging has been suggested as useful for breast density measurements in young women (26, 27) and is currently being used in studies involving young women. However, DXA has many advantages over magnetic resonance imaging or mammography: It is widely available, inexpensive compared with magnetic resonance imaging, already a commonly used and accepted measure for whole-body and regional soft tissue composition, does not entail breast compression, gives results that are objectively interpreted, and uses an X-ray dose 10 times lower than mammography (11).

Disclosure of Potential Conflicts of Interest

No potential conflicts of interest were disclosed.

Acknowledgments

The costs of publication of this article were defrayed in part by the payment of page charges. This article must therefore be hereby marked *advertisement* in accordance with 18 U.S.C. Section 1734 solely to indicate this fact.

We thank all the girls who participated in this study.

Downloaded from cebp.aacrjournals.org on January 16, 2021. © 2008 American Association for Cancer Research.

References

1. Boyd NF, Guo H, Martin LJ, et al. Mammographic density and the risk and detection of breast cancer. N Engl J Med 2007;356:227–36.
2. Boyd NF, Jensen HM, Cooke G, Han HL, Lockwood GA, Miller AB. Mammographic densities and the prevalence and incidence of histological types of benign breast disease. Reference Pathologists of the Canadian National Breast Screening Study. Eur J Cancer Prev 2000;9:15–24.
3. Boyd NF, Lockwood GA, Martin LJ, et al. Mammographic densities and breast cancer risk. Breast Dis 1998;10:113–26.
4. Wolfe JN. Breast patterns as an index of risk for developing breast cancer. Am J Roentgenol 1976;126:1130–9.
5. American College of Radiology. Breast imaging reporting and data system (BI-RADS). Reston (VA): American College of Radiology; 1993.
6. Wolfe JN, Saftlas AF, Salane M. Mammographic parenchymal patterns and quantitative evaluation of mammographic densities: a case-control study. Am J Roentgenol 1987;148:1087–92.
7. Byng JW, Boyd NF, Fishell E, Jong RA, Yaffe MJ. The quantitative analysis of mammographic densities. Phys Med Biol 1994;39:1629–38.
8. Kopans DB. Basic physics and doubts about relationship between mammographically determined tissue density and breast cancer risk. Radiology 2008;246:348–53.
9. Weaver CM, McCabe LD, McCabe GP, et al. Bone mineral and predictors of bone mass in white, Hispanic, and Asian early pubertal girls. Calcif Tissue Int 2007;81:352–63.
10. Laskey MA. Dual-energy X-ray absorptiometry and body composition. Nutrition 1996;12:45–51.
11. Shepherd JA, Kerlikowske KM, Smith-Bindman R, Genant HK, Cummings SR. Measurement of breast density with dual X-ray absorptiometry: feasibility. Radiology 2002;223:554–7.
12. Shepherd JA, Herve L, Landau J, Fan B, Kerlikowske K, Cummings SR. Novel use of single X-ray absorptiometry for measuring breast density. Technol Cancer Res Treat 2005;4:173–82.
13. Novotny R, Going S, Teegarden D, et al. Hispanic and Asian pubertal girls have higher android/gynoid fat ratio than whites. Obesity (Silver Spring) 2007;15:1565–70.
14. Shepherd JA, Herve L, Landau J, Fan B, Kerlikowske K, Cummings SR. Clinical comparison of a novel breast DXA technique to mammographic density. Med Phys 2006;33:1490–8.
15. Tanner JM. Growth at adolescence, with a general consideration of the effects of hereditary and environmental factors upon growth and maturation from birth to maturity. 2nd ed. Oxford: Blackwell Scientific Publisher; 1962.
16. Duke PM, Litt IF, Gross RT. Adolescents' self-assessment of sexual maturation. Pediatrics 1980;66:918–20.
17. Gluer CC, Blake G, Lu Y, Blunt BA, Jergas M, Genant HK. Accurate assessment of precision errors: how to measure the reproducibility of bone densitometry techniques. Osteoporos Int 1995;5:262–70.
18. Shewhart W. Statistical method from the viewpoint of qaulity control. Washington (DC): Graduate School of the Department of Agriculture; 1939.
19. Irwin ML, Aiello EJ, McTiernan A, et al. Physical activity, body mass index, and mammographic density in postmenopausal breast cancer survivors. J Clin Oncol 2007;25:1061–6.
20. Barlow WE, White E, Ballard-Barbash R, et al. Prospective breast cancer risk prediction model for women undergoing screening mammography. J Natl Cancer Inst 2006;98:1204–14.
21. Loughry CW, Sheffer DB, Price TE, et al. Breast volume measurement of 598 women using biostereometric analysis. Ann Plast Surg 1989;22:380–5.
22. Hussain Z, Roberts N, Whitehouse GH, Garcia-Finana M, Percy D. Estimation of breast volume and its variation during the menstrual cycle using MRI and stereology. Br J Radiol 1999;72:236–45.
23. Boyd NF, Lockwood GA, Byng JW, Little LE, Yaffe MJ, Tritchler DL. The relationship of anthropometric measures to radiological features of the breast in premenopausal women. Br J Cancer 1998;78:1233–8.
24. Preston DL, Mattsson A, Holmberg E, Shore R, Hildreth NG, Boice JD, Jr. Radiation effects on breast cancer risk: a pooled analysis of eight cohorts. Radiat Res 2002;158:220–35.
25. Santen RJ, Boyd NF, Chlebowski RT, et al. Critical assessment of new risk factors for breast cancer: considerations for development of an improved risk prediction model. Endocr Relat Cancer 2007;14:169–87.
26. Boston RC, Schnall MD, Englander SA, Landis JR, Moate PJ. Estimation of the content of fat and parenchyma in breast tissue using MRI T1 histograms and phantoms. Magn Reson Imaging 2005;23:591–9.
27. van Engeland S, Snoeren PR, Huisman H, Boetes C, Karssemeijer N. Volumetric breast density estimation from full-field digital mammograms. IEEE Trans Med Imaging 2006;25:273–82.

Downloaded from cebp.aacrjournals.org on January 16, 2021. © 2008 American Association for Cancer Research.

Cancer Epidemiology, Biomarkers & Prevention

AACR American Association for Cancer Research

Breast Density Assessment in Adolescent Girls Using Dual-Energy X-ray Absorptiometry: A Feasibility Study

John A. Shepherd, Serghei Malkov, Bo Fan, et al.

Cancer Epidemiol Biomarkers Prev 2008;17:1709-1713.

Updated version	Access the most recent version of this article at: http://cebp.aacrjournals.org/content/17/7/1709

Cited articles	This article cites 24 articles, 4 of which you can access for free at: http://cebp.aacrjournals.org/content/17/7/1709.full#ref-list-1
Citing articles	This article has been cited by 2 HighWire-hosted articles. Access the articles at: http://cebp.aacrjournals.org/content/17/7/1709.full#related-urls

E-mail alerts	Sign up to receive free email-alerts related to this article or journal.
Reprints and Subscriptions	To order reprints of this article or to subscribe to the journal, contact the AACR Publications Department at pubs@aacr.org.
Permissions	To request permission to re-use all or part of this article, use this link http://cebp.aacrjournals.org/content/17/7/1709. Click on "Request Permissions" which will take you to the Copyright Clearance Center's (CCC) Rightslink site.

Downloaded from cebp.aacrjournals.org on January 16, 2021. © 2008 American Association for Cancer Research.